# SIZE-FREQUENCY DISTRIBUTIONS OF ROCKS ON MARS AND EARTH ANALOG SITES: IMPLICATIONS FOR FUTURE LANDED MISSIONS

M. Golombek and D. Rapp

Jet Propulsion Laboratory
California Institute of Technology
Pasadena, CA 91109

Submitted, February 12, 1996, to
Journal of Geophysical Research, Planets
Special Mars Pathfinder Issue
Revised October 19, 1996

ABSTRACT

The size-frequency distribution of rocks at the Viking landing sites and a variety of rocky locations on the Earth that formed from a number of geologic processes all have the general shape of simple exponential curves, which have been combined with remote sensing data and models on rock abundance to predict the frequency of boulders potentially hazardous to future Mars landers and rovers. Rock data from the near field of the Viking landers where dimensions can be measured accurately in stereo images and estimates from (he far field of Viking 1 have convex up curved shapes on log-log graphs of cumulative frequency per square meter or cumulative fractional area versus diameter. The rock data show a sharp drop-off at large diameters and a progressive approach to a plateau with decreasing diameter (approaching, the total rock coverage), which can be fit well with simple exponential functions. Similar shaped size-frequency distributions of rocks arc found at a wide variety of rocky surfaces on the Earth and can be fit well with simple exponential functions. This distribution is compatible with fracture and fragmentation theory, which provides a physical basis for its wide application. A combined fit to rock area data at both Viking sites was made with a general exponential function, in which the pre-exponential is the total area covered by rocks. Simple linear height versus diameter relationships were also derived from height-diameter ratios at the Viking sites, which suggest that rockier areas on Mars have higher standing rocks than less rocky areas. Height was then substituted into the general exponential function derived for diameter, yielding the cumulative fractional area of rocks versus height for any given total rock coverage on Mars. Results indicate that most of Mars is rather benign with regard to hazards from landing on large rocks. For total rock coverage of 8%, equivalent to modal rock coverage on Mars and the Viking 1 site without the outcrops, about 1 % of" the surface is covered by 20 cm or higher rocks. A lander designed to accommodate landing on 0.5 m high boulders, such as the Mars Pathfinder airbag system, could land on a surface covered by about 20% rocks, similar to the Viking 2 site (which is rockier than -95% of the planet), with -1% of the surface covered by rocks of 0.5 m or higher.

## INTRODUCTION

Predicting the size-frequency distribution of rocks at different locations on Mars is difficult owing to the limited data set (ground truth from only two small sites at the surface) and yet is critical for determining potential hazards for future Mars landers. In this paper, the size-frequency distribution of rocks arc reviewed at the two Viking landing sites with special reference to larger rocks that could be hazardous to a lander. The data arc described in terms of simple mathematical expressions which provide an approximate means of extrapolation to any location on Mars from relationships between the rock frequency curves and remote sensing data. The extrapolations provide a ready mechanism for predicting the size frequency of rocks at any location on Mars for which the total rock coverage is known, which can be used for calculating the probability of a hazardous landing for any proposed landing system. The sim-frequency distributions of rocks at a variety of rocky sites on the Earth arc also presented and it is found that there is considerable similarity to the distributions found on Mars. Results of this work imply that Mars is actually a relatively benign environment with respect to hazards of landing on large rocks for the Mars Pathfinder mission,

## SIZE-FREQUENCY DISTRN3UTIONS OF ROCKS ON MARS

### Background

Plots of the distribution of rocks versus diameter at the two Viking landing sites have been used to suggest a power-law distribution [Binder et al., 1977; Moore et al., 1979], which has been used historically in the analysis of crater and rock siz,c-frequency distributions on the Moon [e.g., Shoemaker and Morris, 1969; 1 lutton, 1969; Moore et al., 1969]. Moore and Keller [199 1 ] suggested that power-law functions could be used to describe rock populat ions for diameters greater than 0.1 m, in the absence of more detailed data on rock populations on Mars. As a result, the following relationships have been used by the engineering community to estimate

the size-frequency relation and fractional area covered by rocks on Mars [e.g., Moore, 1988; Moore and Jakosky, 1989; Moore and Keller, 1991].

$$N(D) = K D^{-2.66} \quad (1)$$

and

$$F(D) = C D^{-0.66} \quad (2)$$

where N(D) is the cumulative number of rocks pcr square meter with diameter greater than or equal to a given diameter D (where D is in meters), F(D) is the cumulative fractional area covered by rocks of a given diameter or larger and C and K arc constants, which arc derived from the cumulative number or area of rocks greater than or equal to 10 cm size. For the Viking 2 site, K is 0.013 and C is 0.0408 [Moore rind Jakosky, 1989]. Moore and Keller [1991] even suggested that C could be fit to the thermal inertia rock abundance estimates by Christensen [1986] for any location on Mars.

Analysis of Viking Data

In general, the data on occurrence of various rock diameters may bc plotted as histograms of number of rocks at each site at each diameter (diameters arc average of length and width, measured to nearest cm) as shown in Figures 1 and 2 (data are from Moore and Keller 11990, 1991 ] for over 400 rocks over areas of -84 $m^2$ from stereo measurements at the Viking sites, without the large, flat and benign outcrops at the Viking 1 site). 1 lowever, in this paper where wc arc primarily concerned with estimating potential landing hazards for future Mars landers, it is more valuable to deal with the cumulative number of rocks per square meter versus rock diameter and the cumulative fractional area covered by rocks versus diameter, integrating from the largest to smallest rock sizes. In this form, the number of rocks (or fractional area of recks) greater than any diameter provide the critical information needed for landing hazard analysis and has been a common representation in the scientific literature [Moore et al., 1979; Malin, 1988, 1989].

Figures 2 and 3 show that Moore's equation 1 dots a reasonably good job of fitting the number versus diameter relationship for reek diameters greater than about 0.2 m at the Viking 2

site, but the power law overestimates the number of rocks at smaller diameters. Even though the power law appears to fit the data for diameters greater than 0.2 m, closer inspection of the data for the larger rock sizes (diameters greater than 0.4 In at Viking 1 and greater than 0.6 m at Viking 2) reveals that the slope of these data points is much steeper than the power law function, so that extrapolating the power law function to larger sizes will overestimate the number of large rocks.

In Figure 4, the cumulative fractional area covered by rocks of a given size or large.r is plotted against diameter along with the power-law function suggested by Moore (equation 2) for the Viking 2 site. The data for either landing site clearly do not follow a straight line and the misfit with the power-law of equation 2 is severe at large and small rock diameters. Over the range of rock diameters from 0.2 to 0.4 m, the power law function provides a reasonable fit to the data. 1 lowever, the power law significant] y overestimates the cumulative area covered by rocks larger than 0.4 m diameter, which is of primary importance in determining the probability of a hazardous landing, and overestimates the cumulative area of rocks smaller than about 0.2 m.

The shapes of the cumulative area curves described by the data appear real and cannot bc made into a straight line; there are not enough small rocks and the area covered by thcm is too little to make up for the deficiency at small reek diameter, and there are too few large diameter rocks at tbc two Viking sites. Even adding smaller rocks (less than about 0.2 m diameter) potentially covering up to an additional 4% of the surface [Moore and Keller, 1991] or rocks potentially shadowed by large rocks beyond a few meters from the lander cannot steepen the curve enough to match a straight line. The disparity at small diameters is not important so long as the power law equation is not applied to smal I diameter rocks. I lowever, the disparity at large diameters is very important because the rock areas associated with the large diameters predicted by the power law equation lead to significant areas covered by larger rock sizes. For example, the data for the Viking 2 site suggest less than 1 % of the surface is covered by rocks of 1 m diameter or greater, whereas the power law function suggests almost an order of magnitude greater surface area covered by such large (and potentially hazardous) boulders.

Exponential Size-Frequency Distributions

The size-frequency data for rocks at (he two Viking sites on log-log plots better describe, a curve rather than a straight line defined by a power law [e.g., Malin, 1988, 1989]. These curves can be fit empirically with simple exponential functions, which appear to better describe rock populations in theory and practice (see later discussion),

$$N(D) = L \exp\{-S D\} \quad (3)$$

$$F(D) = k \exp\{-qD\} \quad (4)$$

as shown in Figures 3 and 4. In these equations, 1. represents the total number of rocks of all sizes per square meter, k represents the fraction of surface area covered by rocks of al 1 sizes (total rock coverage), and s and q arc exponents. Least square curve fits arc excellent, with correlation coefficients of 0.96-0.99 for the Viking data, with values of L and s, or k and q given in Figures 3 and 4. These curves have propert ics which parallel the data: 1 ) F(D) approaches a constant (k) as D approaches O; 2) the slope of F(D) increases continually downward as D increases; and 3) at large D, F(D) drops off sharply with increasing D.

Comparison of the exponential curves and the actual data shows that the fit curves actually drop-off more slowly at large sizes than the actual data, and thus predict slightly more area covered by large rocks than is evidenced by the data (Figure 4). This demonstrates that the flexibility of the exponential function is limited. There are only two parameters; the pre-exponential measures the total rock coverage by rocks of all sizes, while the exponent determines the rate of drop-off at large diameters. Note that the fits to the curves indicate that as D approaches O, F]{D) approaches 0.069 and $F_2(D)$ approaches 0.176, which provide estimates of the total rock coverage by rocks of all sizes. Comparison of the exponential fit curves to the data in non-cumulative histogram form show a reasonable fit to the actual number of rocks per diameter bin (Figures 1 and 2). A comparison with the power-law function for Viking 2 (Figure 2), actually shows a slightly better fit than the exponential curves to the data in this form for diameters larger than 0.2 m. Nevertheless, at diameters smaller than 0,2 m, the power-law function significantly over-predicts the number of small rocks present (even if the function is cut

off at 0.1 m diameter as suggested by Moore). Given that the utility of a simple mathematical representation must apply to the data equally well in histogram and cumulative number and fractional area form, the exponential functions more closely represent the rock size-frequency data at the two Viking sites than do power-law functions.

## Relationships Between Cumulative Number and Area Functions

There is a certain mathematical inconsistency in fitting separate exponential curves to both N(D) and F(D) for any site. For any given mathematical form for the N(D) curve, there is a corresponding theoretical F(D) curve, and vice versa. If the dN/dD curve is exponential, it follows that

$$dN(D) = -Ls\, e^{-sD}\, dD \quad (5)$$

$$N(D) = L\, e^{-sD} \quad (6)$$

$$dF(D) = -(\pi/4)\, Ls\, D^2\, e^{-sD}\, dD \quad (7)$$

$$F(D) = (\pi/4)\, L\, e^{-sD} \{ D^2 + 2D/s + 2/s^2 ) \quad (8)$$

If exponential curves are fit to the Viking N(D) data as in equation 6, equation 8 can be used to predict the corresponding F(D) curve. Using the results given in equation 8, we predict F(D) curves as shown in equations 9 and 10.

$$F_1(D) = (3.82)\, e^{-10.98D} \{D^2 + 0.182D + 0.0166] \quad (9)$$

$$F_2(D) = (3.79)\, e^{-6.98D} \{D^2 + 0.28611 + 0.0411) \quad (10)$$

These curves fit the overall shape of the Viking cumulative area versus diameter data reasonably well as shown in Figure 4, although they slightly overestimate the cumulative area of rocks with diameters less than about 0.5 m.

## Viking 1 Far Field

The areas over which accurate stereoscopic measurements could be made of the rock sizes near the sample fields of the robotic arms are very small, resulting in very small samples of rocks at large diameters [Moore and Keller, 1990, 1991]. At Viking 2, the surrounding terrain has fairly low relief, so that it is extremely difficult to extract additional data from the far field. In

addition, large rocks are present within the near field (up to 1 m diameter) and the near and far rock fields appear homogeneous (Figure 5). By contrast, the area surrounding Viking lander 1 slopes toward the lander, making it possible to examine the far field in some detail. In addition, rocks larger than 0.5 m diameter are not present in the near field and the near and far rock fields appear quite heterogeneous (compare the rocky area to the south of the lander in Figure 6 with the drift-covered area to the northeast in Figure 7), with many large rocks present in the far field (note "Big Joe", a 1.5 m diameter rock is only 10 m from lander 1, Figure 7), As a result, an attempt was made to estimate the sizes of rocks in the far field of the Viking lander 1 site to better characterize the number of large diameter rocks.

Estimates of the distances to several rocks in the far field have already been made [lJ.S.G.S., 1982; Liebes, 1982; Moore et al., 1987], particularly those rocks perched on the rims of nearby craters [Morris and Jones, 1980], as well as some notable nearby rocks such as those named "Big Joe" and "Whale". In addition, the distances of rocks in the near field are known and could be identified in the photographs. Using these far and near field distance estimates, rough radial contours of distance were drawn on the lander image mosaics and a visual search was made for- all large rocks in the extended field. The distance est i mate was used to determine the largest dimensions of rocks from their measured apparent angular widths. The apparent maximum angular width is the total width of the. rocks in silhouette, and usually included more than one face of a rock. The actual dimensions of a rock depend on the angle at which the rock is oriented rel at ive to the cameras, For example, for rocks oriented at 45° the apparent width wili include 0.707 times the sum of the lengths of two sides, and for rocks oriented at 60° it is 0.866 times the length of one side plus 0.5 times the length of the other side. Because separate length and width could not be distinguished for far field rocks, rock "diameter" was taken as roughly 0.75 of the apparent maximum width. A total of 84 apparently large rocks were measured. Only the 17 largest rocks, with diameters greater than 0.8 m, were retained, as the survey is undoubtedly incomplete for smaller rocks. The effective area covered is roughly 20,000 $m^2$ (Figure 8).

The location of large rocks in the far field of the Viking 1 site is shown in Figure 8. It can be seen that many of the largest rocks are concentrated near the rim of crater C, implying that the largest rocks in the far field are ejecta. Figures 3 and 4 show the cumulative number and area versus diameter data for both the Viking 1 near and far fields. Data were plotted for a 2000 $m^2$ rectangle surrounding the large rocks at the rim of crater C and the sum of the near field plus the remaining far field rocks in the 18,000 $m^2$ beyond the rim of crater C. To first order, given the inherent uncertainties in estimating the sizes of rocks in the far field (estimated error in angular width ±5%, estimated error in distance ±25%, estimated error in diameter ±30%), the similarity between the estimated frequency and area of all large rocks is rather similar to that predicted by the exponential fit to the near field data at these larger diameters. The far field area data without the 2000 $m^2$ crater rim is even more similar to that predicted by the exponential fit to the near field data, Note that if rocks smaller than about 0.2 m diameter were added to the near field data (covering up to 4% area as estimated by Moore and Keller [1990]), a worse fit to the larger diameter rocks would result, which is the primary focus of this work. In any case, the distributions are far below those predicted by the power-law functions (equations 1 and 2) at these large sizes. The 2000 $m^2$ area around the crater rim appears to have a greater frequency and area of' large rocks, but nothing is known about the frequency of smaller rocks in this restricted area, so it cannot be used to test the complete size-frequency rock distribution. At these large sizes alone, however, the rock distributions appear similar to those measured near large impact craters on the Moon (Moore et al., 1969; Hutton, 1969; Cintala and McBride, 1995).

## EARTH ANALOG ROCK SIZE-FREQUENCY DISTRIBUTIONS

In this section, the distributions of rock sizes found on Mars are compared with distributions of rock sizes for a variety of rocky sites on the Earth, including: the Ephrata Fan, in the Channeled Scabland of Washington; Mars hill in Death Valley; and volcanic (Goldstone) and alluvial fan (Avawatz) surfaces in the Mojave Desert (data are summarized in Table 1). These surfaces are very rocky by nominal Earth standards. At each site a homogeneous area,

t ypically 10 to 15 m on a side, was surveyed (staked) and all rocks in the area were measured systematically (each measured rock was marked with chalk). Two or three sub-areas within each site were typically measured separately to look for inhomogeneities in the rock distributions; unusually large rocks relative to the areas measured were avoided for this reason (see GDB 1, MEJ NE/NE/SE and NW/SE/SW where one or two large rocks slight] y skew the distributions). At most sites, the length, width and height of each rock were measured down to a minimum dimension (t ypically ~1 cm). in general, there is a decrease in number of rocks at the smallest one or two diameters in the measured data, which may represent a selection deficit and is of no consequence, given that the cumulat ive size frequency data have reached a p] ateau before this diameter is reached,

One area extensively surveyed is the Ephrata Fan in eastern Washington, which is a large, 40 km long depositional fan where channelized (Grand Coulee) flood waters catastrophically released from Glacial Lake Missoula, debouched into the Quincy Basin at Soap Lake in the Channeled Scabland [Baker, 1973; Baker and Nummendal, 1978]. This channel-fan arrangement is analogous to Arcs Vallis and the Mars Pathfinder landing site, where the incised channel debouches onto Chryse Planitia about 100 km south of the landing site [e.g., Golombek et al., this issue]. Rock frequency counts reported in this paper arc from the proximal coarse rocky surfaces of the Ephrata Fan, restricted to areas within about 10 km of Soap Lake (Figure 9); areas farther down the fan are predominantly sand and gravel. Four sites (sites EF1-3 and 5) arc from armored lag deposits in Rocky Ford Creek, in which rocks deposited in the fan arc significant l y concentrated by the removal of fines due to late stage drainage of the Quincy Basin [Baker, 1972], The other three sites arc less rocky surfaces on top of the fan and appear to have had more glacial loess deposited on them (silt mounds common).

A number of sites in eastern California were studied, particularly four areas of Mars Hill in Death Valley (Figure 10). Mars Hill is an abandoned alluvial fan on the eastern side of Death Valley that has had much of the surface fines washed away, leaving an armored rocky surface. Mars Hill (Figure 10) has long been referred to and used as a possible Earth analog since the

earliest Viking lander work [e.g., Mutch et al., 1977], even though virtually no data have been collected to support this assertion. Two areas were measured in the field (MH NE/NE/SE and NW/SE/SW) with the length, width and height of all rocks >7 cm diameter cataloged. Approximately 1000 rocks (down to about 5 cm diameter) were measured on vertical air photos of roughly 1:100 scale at two other areas (MH NE/SE/SW and SE/NE/NE).

Rocky surfaces at two other areas in the eastern Mojave Desert were also measured. Avawatz is from the apex of an active alluvial fan on the eastern side of the Avawatz Mountains, a currently uplifting range in the Mojave Desert. The Goldstone surfaces, in contrast, are from eroded volcanic surfaces in the JPL/NASA Goldstone Deep Space Network tracking facility. Sites GDB 1 (Figure 11) and GDB2 are from the top of a Miocene basalt mesa in which blocks have moved slightly with sediment and dust filling in between. Site GDT3 is a Miocene tuff breccia that was likely deposited as a debris flow, with large (up to 2 m diameter) rhyolite blocks (McConnell et al., 1994). The tuff has been preferentially eroded leaving the rhyolite blocks on the surface with sand and dust filling in between [D. MacConnell, 1995, pers. comm.].

Figures 12 and 13 show the cumulative number and area of rocks versus diameter, respectively, for a representative subset of the rocky surfaces described above, as well as the Viking sites for reference. The total rock coverage varies from 2-60% for the Ephrata Fan, 7,5-25% for Mars Hill, and 10-60% for the eastern California sites. Even so, rock distributions for the Earth sites have very similar shapes to the Viking sites (convex up), with a shallowing in the cumulative number or area at small rock diameters and a sharp drop-off at large diameters, The data from Mars Hill indicate that it is indeed a reasonable analog for the Viking sites. Rocks at Mars Hill, however, have greater height/diameter ratios compared with rocks from the Viking sites on Mars (0.6 versus 0.36 and 0.5, see next section), so that Mars Hill actually represents a more severe testing environment for rovers than appears to be likely for similarly rocky areas on Mars. Data from all the Earth sites can be fit very well (correlation coefficients >0.90) with simple exponential functions (Table 1). The fits to all the sites combined at Mars Hill and the Ephrata Fan, indicate that the Ephrata Fan data tend to drop-off more slowly at large diameter

than do Mars Hill and the Viking sites. This is due to the relative scarcity of smaller rocks at the Ephrata Fan sites compared to the Viking and Mars Hill sites, which produces lower intercepts at small diameters for the Ephrata Fan (e.g., Figures 12 and 13). As a result, the curves for the Ephrata Fan sites appear to be shifted to the right (to larger diameter rocks), which can be explained by the locss covering most small rocks and partially covering large rocks of the proximal Ephrata Fan sites; note that height/diameter ratios support this interpretation, varying from 0.2 for the least rocky site (EF 6) to 0.5 for the rockiest site (EF 3).

Malin [1989] plotted rock size-frequency distributions from 6 different rocky surfaces on the Earth, including Icelandic catastrophic outflow deposits, Antarctic dry valley wall talus, and Hawaiian volcanic ejecta. All areas he counted show the same shaped distribution of cumulative fractional area covered by rocks versus diameter as was found at the Viking landing sites and the Earth sites described in this paper. Even though the geologic processes responsible for the formation of these surfaces appear to be different, the cumulative area versus diameter data on log-log plots show the same shallow slopes at small diameter followed by steeper slopes at larger diameters. The shape of the curves is real and not an artifact of the counting technique because Malin included sieve analysis of smaller rocks down to 1 cm diameter to accurately capture all size rocks.

## EARTH AND MARS ROCK SIZE-FREQUENCY DISTRIBUTION RELATIONSHIPS

The similarity in shape of" rock size-frequency distributions at a variety of rocky surfaces on the Earth and the Viking sites on Mars and the excellent fits of these distributions by simple exponential functions can be explained by simple fracture and fragmentation theory. A wide body of observational data has suggested that the size-distribution of materials (typically at small sizes) expected from fracture and fragmentation would follow an exponential [e.g., Rosin and Rammler, 1933; Gilvarry and Bergstrom, 1961]. This distribution results from the fragment sizes expected from Griffith's fracture criteria, in which failure occurs from propagation of ubiquitous flaws and/or cracks in the material [e.g., Gilvarry, 1961], The theory predicts that the likelihood

of finding boulders without flaws that would lead to break up into smaller pieces decreases exponentially with increasing size. An alternate approach includes subsequent fragmentation due to transport of materials [ Wohletz et al., 1989; Brown and Wohletz, 1995]. This fits well with the observed ubiquity of joints and fractures in geological materials that would tend to break rocks into meter sized and smaller blocks during weathering and transport [e.g., Pollard and Aydin, 1988; Ladeira and Price, 198 J; Tanaka and Golombek, 1989; Crumpler, 1996]. Note that even though power laws have been used to correlate the distribution of rock sizes for a limited range of diameters of rocks from the Moon and around impact craters on the Earth [e.g., Shoemaker and Morris, 1969; Hutton, 1969; Moore et al., 1969; Hartmann, 1969], it seems theoretically unreasonable to expect that the power law extends to large or small diameters, because it would predict ever increasing numbers of smaller and smaller particles and many large particles, which arc neither observed [e.g., Bagnold and Barndorff-Nielsen, 1980; Garvin et al., 1981] nor predicted [Gilvarry, 1961].

Because the theory is fairly independent of geologic process, it can explain the size distribution of rocks observed. On Mars, the rocks at the Viking 1 site arc thought to be a partially covered and eroded lava flow surface,' although ejecta from craters and flood deposits have also been suggested from the apparent diversity of rock types at this site [Binder et al., 1977]. Viking 2 rocks arc likely cjc.eta from the nearby large crater Mie [Mutch et al., 1977]. The Earth sites formed from a wide variety of geologic processes, yet all distributions can be fit well by simple exponential functions. The size-frequency distribution may follow a slightly more complicated exponential function in which the diameter in equations 3 and 4 is raised to soInc power n, which is a form of a Weibull distribution [ Wohletz et al., 1989; Brown and Wohletz, 1995]. These function parallel simple exponentials, except that they drop-off more sharply at large diameter for n>1. As mentioned earlier, there is some evidence for this behavior at the larger diameters in the Viking and Earth cumulative area distributions (Figures 4 and 13). However, the fact that simple exponential.s alone provide excellent fits to the data (correlation

coefficients >0.9) suggests that if a best fit were made to an exponential of argument $D^n$, the power n would not range far from onc for most sites.

## GENERALIZED EXPONENTIAL CURVES AND DIAMETER-HEIGHT RELATIONSHIPS

The Viking data, as well as data from various Earth sites suggest that the curves of fraction of surface covered by rocks with diameters equal to or greater than some value D for various total rock coverage fractions might be expressible in the general form:

$$F_k(D) = k \exp\{-q(k) D\} \quad (11)$$

in which k is the cumulative fraction of surface covered by rocks of all sizes or the total rock coverage, and q(k) is the exponential factor, which defines the rate of drop-off in the exponential function at large rock diameters. For Viking landers 1 and 2, the best fits to the data are q(0.069) = 4.08 and q(O. 176) = 2.73, respectively. If wc assume that there is a smooth variation in the $F_k(D)$ curves from one value of k to another, wc can extrapolate these results to other values of k. To do this, wc must first seek an equation to define q as a function of k. Clearly, q must decrease as k increases, because the family of curves $F_k(D)$ pushes upward and to the right as k increases. We define a function of the form shown in equation 12, and fit this to the two points corresponding to the Viking sites.

$$q(k) = (A + B/k) \quad (12)$$

After fitting to the Viking data, the result was q(k) = (1.79 -t-O. 152/k). This function satisfies the requirement that it gives the correct values of q(k) for the two Viking sites, although a variety of other similar functions would produce virtually the same result because the extrapolation of k occurs over a very small range (0.02-0.3). Indeed other functions have been tried and tile.y produce only modest changes in the family of curves of $F_k(D)$ for various k. This family of curves is non-crossing, and of similar shape, as wc have observed for the Viking sites and a variety of Earth sites as well (Figure 14).

For the Viking sites, the height of each rock was plotted against diameter in Figure 15. The linear least-squares best fit at Viking lander 1 for the near field data is:

$$H = 0.365\ D + 0.008 \quad (13)$$

which is identical to the fit for the near and far field data combined, and the best fit at Viking lander 2 is:

$$H = 0.506\ D + 0.008 \quad (14)$$

showing that rocks at the Viking 1 site have heights that average to -3/8 their diameter, and at the Viking 2 site the heights average to - I/2 their diameter. We can convert from the indcpcndcnt variable D to the independent variable H using a generalized relationship between H and D.

$$H = (0.25 + 1.4\ k)\ D \quad (15)$$

Note that in addition to matching the observed average height diameter ratios at the two Viking sites, H/D is estimated to be 2./3 when k = 0.3. Thus equation 15 is a relationship that forces the H/D ratio to vary from 0.32 for a relatively rock-free area with k = 0,05, to 0.67 for a very rocky area with k = 0.30. This implies that rocks at rockier sites tend to be higher (relative to their diameters) than rocks at less rocky sites, which effectively simulates progressive burial of rocks at less rocky sites by sand and dust [e.g., Christensen and Malin, 1993]. Equation 15 therefore embodies the concept that the burial of rocks by fine material is more extensive at less rocky sites, Inverting equation 15 and substituting into equation 11, wc obtain an expression in terms of H:

$$F_k(H) = k \exp\{-p(k) H\} \quad (16)$$

in which p(k) = (1.79 + O. 152/k)/{0.25 + 1.4 k}. The curves of1~~(11) for various k are as shown in Figure 16, The expressions for F(H), like those for F(D), arc conservative estimates in that they overestimate the height of large rocks at the Viking sites. Figure 16 demonstrates, however, that at the Viking 1 site, less than 0.1 % of the surface is covered by the highest rock of only 0.2 m. At the Viking 2 site, the highest rock is 0.5 m, covering lcss than 1 % of the surface.

## RELATIONSHIP OF VIKING LANDER DATA TO OTHER AREAS ON MARS

### Background

Even though the size-frequency distribution of rocks on Mars has been determined directly only at the two small Viking landing sites, remote sensing data have been used to model rock abundances on Mars, Specifically, the Viking infrared thermal mapper (IRTM) observations have been used to determine the surface rock abundances over broad 10 latitude by 10 longitude areas on Mars [Christensen, 1986]. The rock abundances are calculated from the temperature contrasts in the measured bands of the IRTM. Results indicate total abundance or surface area of rocks greater than 10-15 cm diameter versus fine component materials such as soil, dust or sand [e.g., Moore and Jakosky, 1989; Christensen and Moore, 1992] and are believed to be accurate to about 20% [Christensen and Malin, 1993]. Rock abundances calculated in this fashion indicate a unimodal Poisson distribution over the planet with minimum abundances of 1%, maximum abundances of 30% and a mode of about 6%. To first order, most of Mars is relatively free of rocks, although no areas on Mars are totally rock free on the scale of the IRTM measurements. In contrast, the Viking landing sites are uncharacteristically rocky sites on Mars, with the IRTM measurements indicating that Viking 1 and 2 are in the 50th and -95th percentile of rockiness of the planet, respectively [Christensen, 1986; Moore and Jakosky, 1989; Christensen and Moore, 1992],

Extrapolation of IRTM rock abundances at the scale of tens of kilometers to rock frequency distributions at a scale of less than a meter is highly uncertain. It is not known if a rock abundance indicated by the IRTM measurements represents a series of benign outcrops (e.g., over 4% of the surface of the Viking 1 site) or a distribution of hazardous rocks. Nevertheless the approach has been suggested previously in the literature [e.g., Moore and Jakosky, 1989] and has been used by the engineering community. Given these large uncertainties, we believe our model rock abundances are reasonable and conservative estimates for the following reasons. First, the exponential function used to model the distributions is common to surfaces formed from a wide variety of processes and is expected from basic failure and transport theory [Gilvarry, 1961;

Wohletz et al., 1989]. Second, model abundances assume that all of the IRTM rock abundances are composed of hazardous rocks (no outcrops). Third, model abundances drop-off more slowly at large diameter than the actual data (e.g., compare the total Mars Hill and Ephrata Fan exponential fits with individual site data in Figure 13 and the Viking site data in Figures 14 and 16). Lastly, deviations of individual site data (Figures 4 and 13) from the model predictions of moving up and to the right with increasing k on Figures 14 and 16, are toward faster drop-offs at larger diameters with increasing k rather than slower drop-offs.

Model Rock Abundance Distributions on Mars

If we can make the rather far-reaching assumption that the Viking rock frequency distributions are representative of genera] rock frequency distributions on Mars, then the derived rock abundance from the IRTM data for any site on Mars can be used to identify the total cumulative fractional area of rocks (i.e., the left hand side of the cumulative area versus diameter curves). This is consistent because the rock abundances arc determined for 10 cm and larger blocks on the surface. At this diameter, the cumulative fractional area versus diameter plots tend to flatten out, approaching their total fractional area of rock coverage at smaller diameters (Figure 4). As a result, wc can usc the rock abundance from the thermal inertia data (Christensen, 1986) as k in equation 11 and derive q(k) from equation 12 for any rock abundance value, thereby allowing us to crudely estimate the si?,c-frequency distribution of rocks at any location on Mars.

This calculation is conceptually equivalent to Christensen and Malin's [1993] suggestion that rock abundances on Mars reflect the. thickness of mantling fine material. In this simple model, the maximum rock abundances occur in areas with no mantling sand or dust, and less rocky areas arc mantled by progressively greater thicknesses of dust (up to 1 m thick). The curves shown in Figures 14 and 16 arc derived in the same spirit as this assumption. The maximum rock coverage of -30% rocks is represented by the upper-right curve, which when covered with up to 1 m of dust would produce. the parallel curve in the lower left of about 2% rock coverage. Areas with intermediate rock abundances would behave roughly like those shown

in Figures 14 and 16, namely that as the total rock coverage diminishes, the distribution curves will retain the same generic shape but will move downward and to the left. In addition to the rock abundance changing in this manner, the height of rocks also changes systematically with total rock abundance according to equations 15 and 16 such that rockier areas tend to have relatively higher rocks and less rocky areas tend to have lower rocks measured as fractions of diameters. As a result, our model of rock heights is also consistent with Christensen and Malin's model of sand and dust mantling less rocky areas, thereby decreasing the rock height for any diameter in less rocky areas. These functions and curves define the total size-frequency distribution of rocks on Mars at any location in terms of number, diameter and height, which can be used for engineering assessments of probability y of hazardous landing for a given lander configurate ion.

## DISCUSSION AND CONCLUSIONS

In this paper, the size-frequency distributions of rocks at the Viking landing sites arc analyzed, with special reference to large rocks that could be hazardous to future landers on Mars. The rock data plotted in either cumulative number per square meter or cumulative fractional area versus diameter at both Viking sites have very similar overall shapes, displaying a convex-up curved shape on log-log plots that can be fit very well with simple exponential functions. The rock data do not appear linear on log-log plots over wide ranges of diameter, so that fits using power-law functions (commonly used to fit crater size-frequency data) severely overestimate the frequency and fractional area covered by both large diameter and small diameter rocks. The size-frequency distributions of rocks found at a wide variety of rocky surfaces on the Earth, which formed from an equall y wide variety of geologic processes, appear to have similar overall shapes and can be fit very well with simple exponential functions. Exponential size-frequency distributions are, in fact, predicted from fracture and fragmentation duc to transport theory which provides a physical basis for their wide application.

The consistency of the size-frequency rock distributions found on the Earth and the two Viking landing sites suggests that similar shaped rock size-frequency distributions might be

applicable to other areas on Mars. Fits to the Viking lander cumulative fractional area of rocks versus diameter data were made at both sites with a general exponential function, in which the pre-exponential constant describes the total area covered by rocks at the site and the exponent is rock diameter times a simple function of the pre-exponential constant. Simple linear height versus diameter relationships were also derived at the two Viking sites, which suggest that less rocky areas on Mars have lower height/dianlctcr ratios than rockier areas. Height was then substituted into the general exponential function derived for diameter, which yielded an exponential function describing the cumulative fractional area of rocks versus height.

Viking thermal inertia measurements and models developed by Christensen [ 1986] have been developed to estimate the fractional surface area covered by rocks with high thermal inertia (greater than about 10 cm diameter) versus smaller particles, such as sand and dust, with low thermal inertia. These estimates indicate that rock coverage on Mars in the 10 latitude by 10 longitude remotely sensed areas displays a Poisson distribution, with a mode of only 6% rocks, a maximum of 30%, and a minimum of 1 % rock coverage. Because the cumulative fractional area covered by rocks of 10 cm diameter and larger is fairly close to the total rock coverage, it has been used as the pre-exponential constant in the genera] exponential function fit to the Viking lander rock data to describe the cumulative fractional area versus diameter or height at any location on Mars.

Results indicate that most of Mars is rather benign with regard to hazards from landing on large rocks, The estimates of rock coverage by Christensen [ 1986] suggests that 50% of Mars has rocks covering only 8% or less of its exposed surface. For total rock coverage of 8%, about 1-2% of the surface is covered by 20 cm or higher rocks. The Viking 1 landing site is covered by less than 8% rocks (without the outcrops), so that only 1 -2% of the surface is covered by rocks higher than the clearance (22 cm) provided by its legs [Soffen, 197'7]. Because about 50% of Mars is covered by <8% rock coverage, Viking could have been sent to about half of the surface of Mars with 1 -2% of the surface covered by rocks higher than its surface clearance. In contrast, a lander with a surface clearance of 35 cm could land on a surface covered by 12% rocks, with 1 % of the

surface covered by 35 cm or higher rocks. For this example, roughly 70% of Mars has 12% or less rock coverage. Finally, the Mars Pathfinder lander air bag system is designed to accommodate landing on 0.5 m high boulders. Such a landing system could land on a surface covered by about 20% rocks, similar to the Viking 2 site (which is rockier than -95% of the planet), with roughly 1 % of the surface covered by rocks of 0.5 m or higher.

## ACKNOWLEDGMENTS

Wc thank Henry Moore for providing us with electronic copies of the Viking rock data and for many helpful discussions. Roger Bourke got one of us interested in rock frequency counts during the Mars Rover Sample Return Developmental Flight Project and provided data (airphotos from the surveyed area of Mars Hill), encouragement and occasionally misleading advice. Ryan I loffman, Edwin Emmer and Nathan Rich, helped count rocks at Mars Hill and Goldstone and Ryan Hoffman did most of the data reduction of the Ephrata fan and eastern California counts. Dave McConnell was an excellent field guide to the Goldstone surfaces and their geology. Vic Baker introduced one of us to the Channeled Scabland and the Ephrata Fan and Jim Rice and Ken Edgett help 'count rocks on these surfaces. Mike Malin and Phil Christensen cheerfully discussed their data and models. We also thank the reviewers of this paper for comments and for pointing out references. The work described in this paper was carried out at the Jet Propulsion Laboratory, California 1 nstit ute of Technolog y, under contract with the National Aeronautics and Space Administration.

## REFERENCES

Bagnold, R, A., and O, Barndorff-Nielsen, The pattern of natural size (distributions, *Sedimentology,* 27, 199-207, 1980.

Baker, V. R., Paleohydrology and sedimentology of Lake Missoula flooding in eastern Washington, *Geol.* Sot. *America Spin. Pap. 144,73* p., 1972.

Baker, V, R., and D. Nummendal, The Channeled Scabland, NASA, Wash. DC, 186 p., 1978.

Binder, A. B., R. E. Arvidson, E. A. Guinness, K. 1.. Jones, E.C. Morris, '1'. A. Mutch, D.C. Pieri, and C. Sagan, The geology of the Viking lander 1 site, *J. Geophys. Res.,* 82,4439-4451, 1977,

Brown, W. K., and K. H. Wohletz, Derivation of the Weibull distribution based on physical principles and its connection to the Rosin-Rammler and lognormal distributions, J, Appl. Phys., 78,2758-2763, 1995.

Christensen, P. R., The spatial distribution of rocks on Mars, *Icarus,* 66',217-238, 1986.

Christensen, P. R., and M. C. Malin, A simple model of elastic sediments on Mars (abs.), *lunar Planet. Sci. XXIV 285-286,1993.*

Christensen, P. R., and H. J. Moore, The Martian Surface Layer, Chapter 21, p. 686-729 in MAR S., Kieffer, H. H., B. M. Jakosky, C. W. Snyder, and M. S. Matthews, eds., University of Arizona Press, Tucson, 1498 pp, 1992.

Cintala, M. J., and K. M. McBride, Block distributions on the lunar surface: A comparison between measurements obtained from surface and orbital photography, NASA Tech. Mem. 104804,41 pp., October 1995.

Crumpler, L. S., The significance of rock abundances at the Viking lander sites: implications for Mars Pathfinder and Surveyor landers (abs.), *Lunar Planet. Sci. XXVII, 273-274,* 1996.

Garvin, J. B., P. J. Mouginis-Mark, and J. W. Head, Characterization of rock populations on planetary surfaces: Techniques and a preliminary analysis of Mars and Venus, *Moon and Planets,* 24, 355-387, 1981.

Gilvarry, J. J., Fracture of brittle solids 1. Distribution function for fragment size in single fracture (theoretical), *J. Appl. Phys., 32, 391-399, 1961,*

Gilvarry, J. J., and B. H. Bergstrom, Fracture of brittle solids 11. Distribution function for fragment size in single fracture (experimental), *J. Appl. Phys.,* 32,400-410, 1961.

Golombek, M. P., R. A. Cook, H. J. Moore and '1'. J. Parker, Selection of the Mars Pathfinder landing site, *J. Geophys. Res.,* this *volume.*

Hartmann, W. K., Terrestrial, lunar and interplanetary rock fragmentation, *Icarus, 10, 201-213, 1969.*

Hutton, R. E., Lunar surface models, NASA SP-8023, 55pp., 1969.

Ladeira, F. L., and N. J. Price, Relationship between fracture spacing and bed thickness, *J. Struct. Geol., 3,* 179-183, 1981.

Liebes, S., Jr., Viking lander atlas of Mars, NASA Contr. Rep. 3568,250 p., 1982.

MacConnell, D. F., C. McCabe, R. K. Dokka, and M. Chu, Paleomagnetic and structural evidence for localized tectonic rotation associated with fault drag in the northeastern Mojave Desert: implications for the late Cenozoic tectonic evolution of the Eastern California shear zone, *Earth Planet. Sci. Letts.*, 126,207-216, 1994.

Malin, M. C., Rock populations as indicators of geologic processes (abs.), NASA Tech. Mem. 4041, Rep. Planet, Geol. Geophys. Prog. -1987,502-504, 1988.

Malin, M. C., Rock populations as indicators of geologic processes (abs.), NASA Tech. Mem. 4130, Rep. Planet. Geol. Geophys. Prog. -1988,363-365, 1989.

Moore, H. J., Mars Surface Model, in Environment of Mars, 1988, D. Kaplan, cd., NASA Tech. Mem 100470,3-1 to 3-24, October 1988.

Moore, H. J., R. E. Hutton, G. D. Clew, and C. R. Spitzer, Physical properties of the surface materials at the Viking landing sites on Mars, *U. S. Geol. Surv. Prof. Pap. 1.?6'9, 222p.*, 1987.

Moore, H. J., and B. M. Jakosky, Viking landing sites, rcn~otc-sensing observations, and physical properties of martian surface materials, *Icarus, 81, 164-184,* 1989.

Moore, H. J. and J. M. Keller, 1990, Surface-material maps of the Viking landing sites on Mars (abs.), NASA Tech. Mem. 4210, Rep. Planet. Geol. Geophys. Prog. -1990, 160-162.

Moore, H. J. and J. M. Keller, 1991, Surface-material maps of the Viking landing sites on Mars (abs.), NASA Tech. Mem. 4300, Rep. Planet. Geol. Geophys. Prog. -1989,533-535.

Moore, H. J., R. J. Pike, and G. E. Ulrich, Lunar terrain and traverse data for lunar roving vehicle design study, Prelim. U. S. Geol. Surv. Rep., March 19, 1969.

Moore, 11. J., C. R. Spitzer, K. Z. Bradford, P. M. Cates, R. E. Hutton, and R. W. Shorthill, Sample Fields of the Viking Landers, *J. Geophys. Res.*, 84,8365-8377, 1979.

Morris, E. C., and K. L. Jones, Viking 1 lander on the surface of Mars: Revised location, *Icarus,* 44,217-222, 1980.

Mutch, T. A., R, E. Arvidson, A. B. Binder, E. A. Guinness, and E. C. Morris, The geology of the Viking Lander 2 site, *J. Geophys. Res.*, 6'2,4452-4467, 1977.

Pollard, D. D., and A, Aydin, Progress in understanding jointing over the past century, *Geol.* Sot. *Amer. Bull., 100, 1181-12.04,* 1988.

Rosin, P., and E. Rammler, The laws governing the fineness of powdered coal, J. *Inst. Fuel,* 7, 29-36, 1933,

Shoemaker, E. M., and E. C. Morris, Size-frequency distribution of fragmental debris, in Surveyor Program Results, NASA Spec. Pub. 184, pp. 82-96, 1969.

Soffen, G. A., The Viking Project, *J. Geophys. Res.*, 82,3959-3970, 1977.

Tanaka, K. 1.. and Golombek, M. P., Martian tension fractures and the formation of grabens and collapse features at Valles Marineris, *Proc. Lunar Planet. Sci. Conf. 19th,* 383-396, 1989.

U.S. Geological Survey, Viking lander 1 rectified photomosaics, Maps I-1243, 1-1366, 1367, 1368, 1982.

Wohletz, K. H., M. F. Sheridan, and W. K. Brown, Particle size distributions and the sequential fragmentation/transport theory applied to volcanic ash, *J. Geophys. Res.*, 94, 15,703-15,721, 1989.

'1'able 1. Rocky sites measured on Earth.

| Site | 1 ocation | Area ($m^2$) | Sub Areas | No, of Rocks | Total Rock Coverage | k | q(k) | r | Comments |
|---|---|---|---|---|---|---|---|---|---|
| EF1 | T20NR27E S4 NW | 154 | 3 | 293 | 18% | .36 | 1.47 | .93 | 8 mi SSE of SL* |
| EF2 | T20N R27E S9 NE | 334 | 3 | 559 | 26% | .31 | .51 | .95 | 9.5 mi SSE of SL* |
| EF3 | T21N R27E S17 NW | 158 | **4** | 603 | 59% | .65 | .341 | .95 | S mi SSE of S].* |
| EF4 | T21NR27E S7 NW | 373 | 2 | 228 | 3% | .04 | 1.02 | .95 | 3.5 mi S of SL* |
| EF5 | T21N R27E S6 C | 261 | 2 | 504 | 25% | .28 | .36 | .96 | **2.5** mi S of S1.* |
| EF6 | T21NR27E S6 SW | 334 | 2 | 138 | 1.8% | .02 | .90 | .95 | 3 mi S of SL* |
| EF7 | T21N R26E S35 SE | 232 | 2 | 713 | 4.8% | .06 | 1.98 | .94 | 8.5 mi S of SL* |
| MH | NE of SE of SW | 210 | 1 | 1020 | 22% | .29 | .97 | .95 | From Airphoto |
| MH | SE of NE of NE | 210 | 1 | **917** | 10% | .18 | 2.75 | .99 | From Airphoto |
| MH | NE of NE of SE | 149 | 1 | 277 | 7.5% | .12 | 1.9 | .98 | # |
| MH | **NW** of SE of SW | **74** | 1 | 160 | **22%** | .27 | .58 | .99 | # |
| GDB1N | T14N R1E S14 NW | 82 | 1 | 707 | 34% | .51 | 1.64 | .98 | |
| GDB1S | T14N R1E S14 NW | 82 | 1 | 412 | 11% | .31 | 3.89 | .97 | |
| GDB2 | T21N R27E **S6 SW** | 39 | 1 | 391 | **57%** | **1,0** | **1.58** | **.98** | |
| GDT3 | T14N R1E S11 NW | 93 | 2 | **438** | 48% | .60 | .55 | **.96** | |
| Avwtz | T18N R6E S32 SE | 149 | 1 | 80 | >20% | .28 | .89 | **1.0** | ¶ |

* SL = Soap Lake
# MH is at' **36°23' N, 116°51' 15"** W; site location refers to portion of area surveyed during Mars Rover Sample Ret urn Developmental 1 'light Project
¶ only ≥0.3 m Av. Dia. Rocks Measured
k, q(k) from equation (1 1) and r (correlation coefficient) arc from least squares exponential fit to data plotted at each diameter

FIGURE CAP'1'1ONS

Figure 1. Histogram showing number of rocks of each diameter (measured to nearest cm) at Viking lander 1. Binned data and the exponential fit arc also shown, The exact method of binning the data has no effect on the outcome..

Figure 2. 1 listogram showing number of rocks of each diameter (measured to nearest cm) at Viking lander 2. Binned data and the exponential fit arc shown; power law function

suggested by Moore and Jakosky [1989] and Moore and Keller [1990] for rocks greater than 0,1 m diameter at the Viking 2 site is also shown,

Figure 3. Cumulative number of rocks versus diameter of the near fields of the Viking sites and the far field of Viking 1. Least-square exponential curves for every rock at Viking landers 1 and 2 (equation 3); $L_1$=5.61, $s_1$=12.05; $L_2$=6.84, $s_2$=8.30 with correlation coefficients (r) of' 0.99 and 0.98, respectively, indicate excellent fits to the data. Dotted line is exponential fit to Viking 1 near and far field data (L=3.37, s=2.83, r=0.94). Dashed line is exponential fit to near plus far field without the crater rim data (L=3.82, s=3.38, r=0.94). Straight line is a power-law function for Viking lander 2 (equation 1), suggested by Moore and Jakosky [1989] and Moore and Keller [1990] for rocks with diameters greater than 0.1 m.

Figure 4. Cumulative fractional area covered by rocks versus diameter for the near fields of the Viking lander sites and the far field of Viking 1. Least square exponential curves for every rock (equation 4) ($k_1$=0.069, $q_1$=4.08; $k_2$=0.176, $q_2$=2.73), with correlation coefficients of $r_1$ =0.96 and $r_2$=0.99, respectively, indicate excellent fits to the data. Dashed line is exponential fit to Viking 1 near and far field data (k=0.061, q=1.26, r=0.96). Dash-dot-dash line is exponential fit to near plus far field without the crater rim data (k=O.065, q= 1.58, r=0.96). The dotted lines are derived from exponential curve fits to N(D) as shown in equations 9 and 10. Straight line is a power-law function for Viking lander 2 (equation 1) suggested by Moore and Jakosky [1989] and Moore and Keller [1990] for rocks with diameters greater than 0.1 m.

Figure 5. Mosaic of images of Viking lander 2 surface looking towards the northeast. Surface is both of low relief and the rock field is visually homogeneous. Two large, meter diameter rocks (marked LR) are included in the near field data. No attempt was made to extract far field data from the images at Viking lander 2.

Figure 6. Mosaic of images of Viking lander 1 surface looking towards the south. Surface slopes towards the lander so that rocks on the horizon marked LR are about 80 m away,

indicating they arc about 2 m in size. Scene shows a moderately rocky plain with outcrops in the middle distance (OC). The sizes of rocks in the far field were estimated from their apparent distances.

Figure 7, Mosaic of images of Viking lander 1 surface looking towards the northeast. Note the much less rocky appearance and the preponderance of drift material compared with the region to the south (Figure 6). The large boulder in the center of the image is "Big Joe" (BJ); it is 10 m away from the lander and about 1.5 m in diameter. "Whale" (Wh), to the upper right of the scene, is about 2 m in diameter and about 25 m away, These rocks were included in the estimates of far field rock abundance at this site.

Figure 8. Map view of Viking 1 far field showing positions of nearby craters, the small near-field, and positions and diameters of the largest 17 rocks in the far field. Dots, large circles, and rectangles with rounded corners arc rocks of 0.8-0.9 m, 1 .0-1.9 m, and 2.0 m or larger in diameter, respectively.

Figure 9. Photograph of site EF3 on the Ephrata Fan in the Channeled Scabland of eastern Washington where rock size frequency measurements were made, This site is the rockiest part of the proximal portion of the fan (60% of the surface is covered with rocks), where rocks have been significantly concentrated in an armored lag. Note typical (lower) rock concentrations in the distance and the largest rock ("monster rock") carried by the catastrophic flood waters (18 x 11 x 8 m) in the rear right; people (Jim Rice and Ken Edgett) and car for scale.

Figure 10. Surface photograph of rocky portion of Mars Hill in Death Valley, California (over 20% of the surface is covered by rocks). Site has long been considered as an analog for the surface of Mars duc to its stark visual similarity, even though this paper presents the first quantitative data to support this assertion. The surface is an abandoned alluvial fan in which large rocks have been concentrated as a lag by subsequent removal of the finer matrix. Person to the right for scale, Don Bickler is the designer of the Pathfinder microrover mobilit ys ystem.

Figure 11. Surface photograph of site GDB 1 N, which is an eroded Miocene basalt in the Goldstone Deep Space Network complex in the Mojave Desert of eastern California. This area has 34% of its surface covered by rocks, making it much rockier than the Viking 2 site. Note people for scale and chalk marks on measured rocks.

Figure 12. Cumulative number of rocks versus diameter at a representative number of the various Earth analog sites and for the Viking lander sites. The data marked EF Total and MH:TOT arc for the sum of all Ephrata Fan sites and Mars Hill sites and the dashed curve (L=1.44, s=3.96, r= O.98) and solid curve (I .=4.78, s=3.06, r= O.98) arc their exponential fits (to every rock), respectively.

Figure 13. Cumulative fraction of surface area covered by rocks versus diameter for a representative number of the various Earth analog sites and for the Viking lander sites. The data marked EF Total and MH:TOT arc for the sum of all Ephrata Fan sites and Mars Hill sites and the dashed curve (k=0.17, q=0.57, r=0.99) and solid curve (k=0.1 '7, q=0.95, r= 0.99) arc their exponential fits (to every rock), respectively.

Figure 14. Model of curves of cumulative fractional area covered by rocks of diameter D or greater versus diameter corresponding to equation 11 with equation 12 used for q(k). The range of total rock coverage is 0.3,0.2, 0.1, 0.05 and 0.02.

Figure 15. Rock height versus diameter at the near field of the Viking 1 and 2 sites and at the far field of Viking 1. Least squares linear fit is H = 0.365 D + 0.008 (r=0.84) and H = 0.506 D + 0.008 (r=0.78), respectively. Thus the average height of a rock at the Viking 1 and 2 sites is roughly 3/8 and 1/2 of its diameter, respect ively. Adding the far field data to the near field for the Viking 1 site yields the same relation (H= 0.3591) + 0.009, r=O.95).

Figure 16. Family of curves of cumulative fractional area covered by rocks of height H or greater versus rock height corresponding to equation 16. The range of total rock coverage (O. 3, 0.2,0.1,0.05 and 0.02) corresponds to those indicated by thermal inertia data and models.

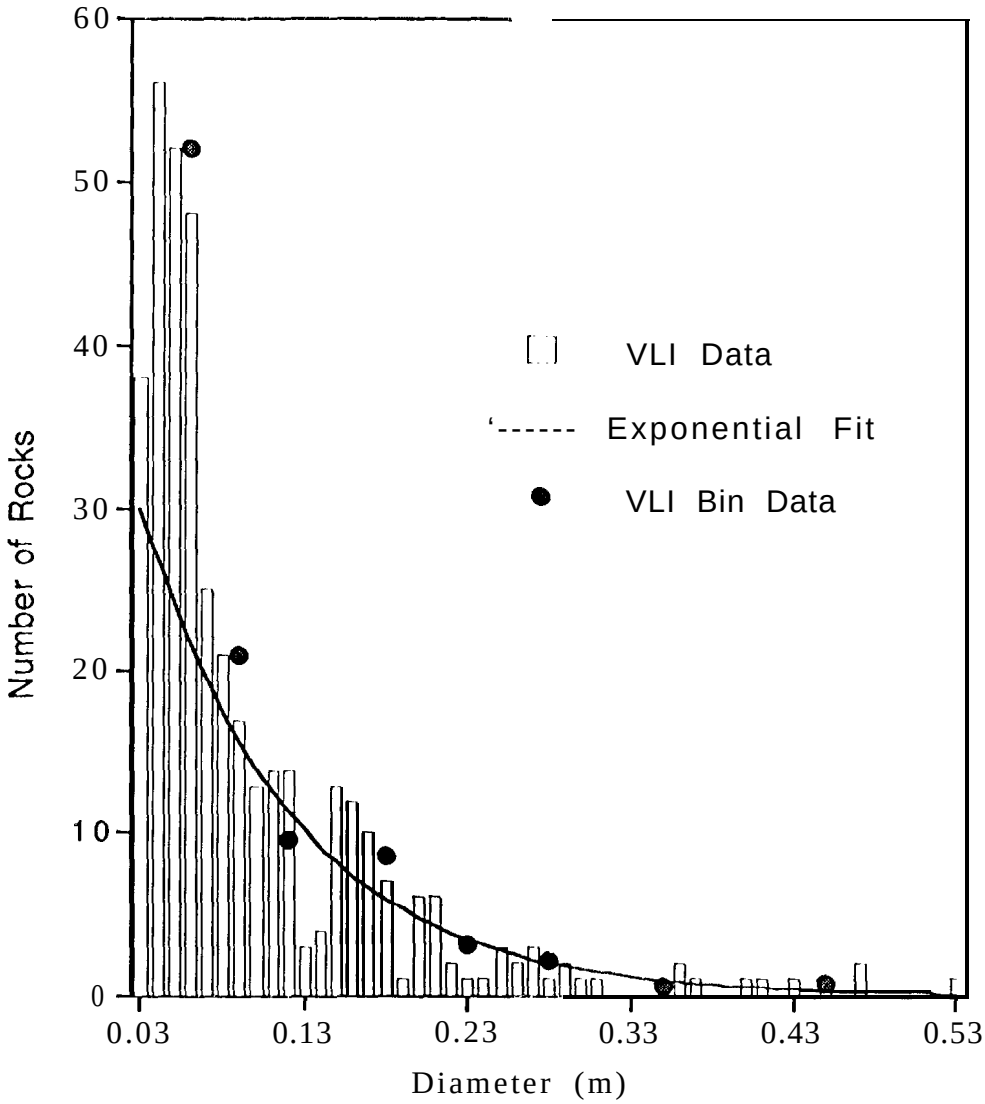
60
50
40
30
20
10
0
Number of Rocks
VLI Data
Exponential Fit
VLI Bin Data
0.03
0.13
0.23
0.33
0.43
0.53
Diameter (m)

Figure 1

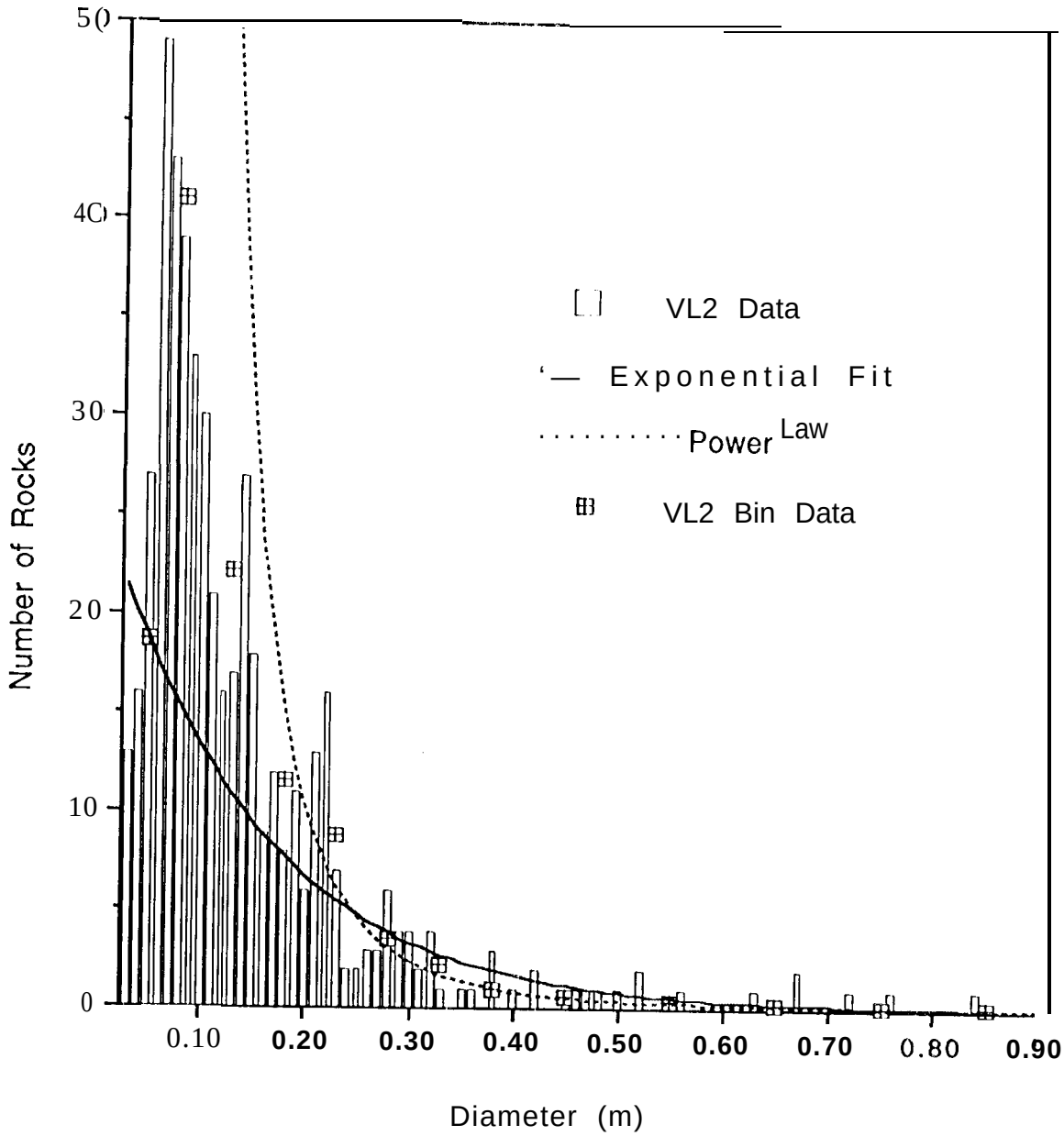
50
40
30
20
10
0
Number of Rocks
VL2 Data
Exponential Fit
Power Law
VL2 Bin Data
0.10
0.20
0.30
0.40
0.50
0.60
0.70
0.80
0.90
Diameter (m)

**Figure 2**

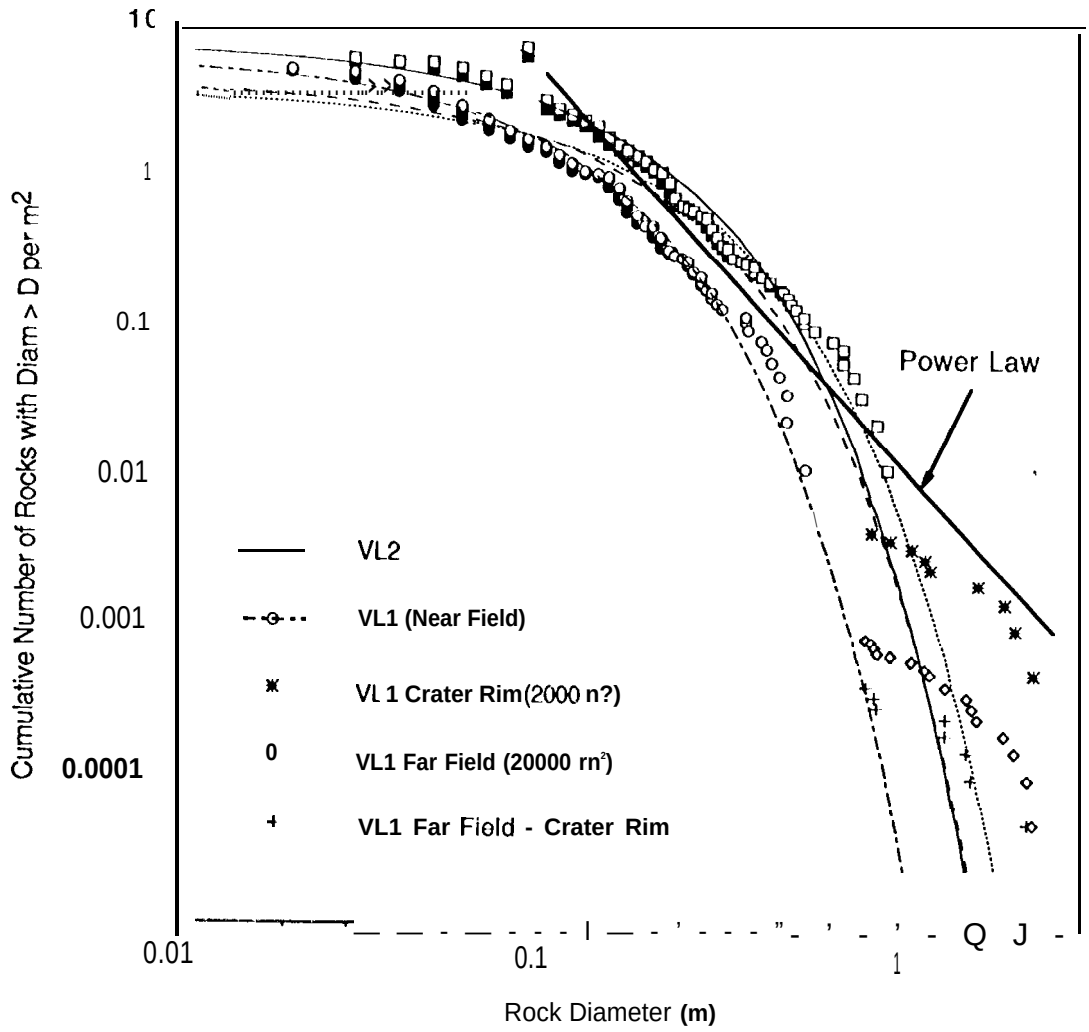
10
1
0.1
0.01
0.001
0.0001
Cumulative Number of Rocks with Diam > D per m2
Power Law
VL2
VL1 (Near Field)
VL 1 Crater Rim(2000 n?)
VL1 Far Field (20000 rn²)
VL1 Far Field - Crater Rim
0.01
0.1
1
Rock Diameter (m)

Figure 3

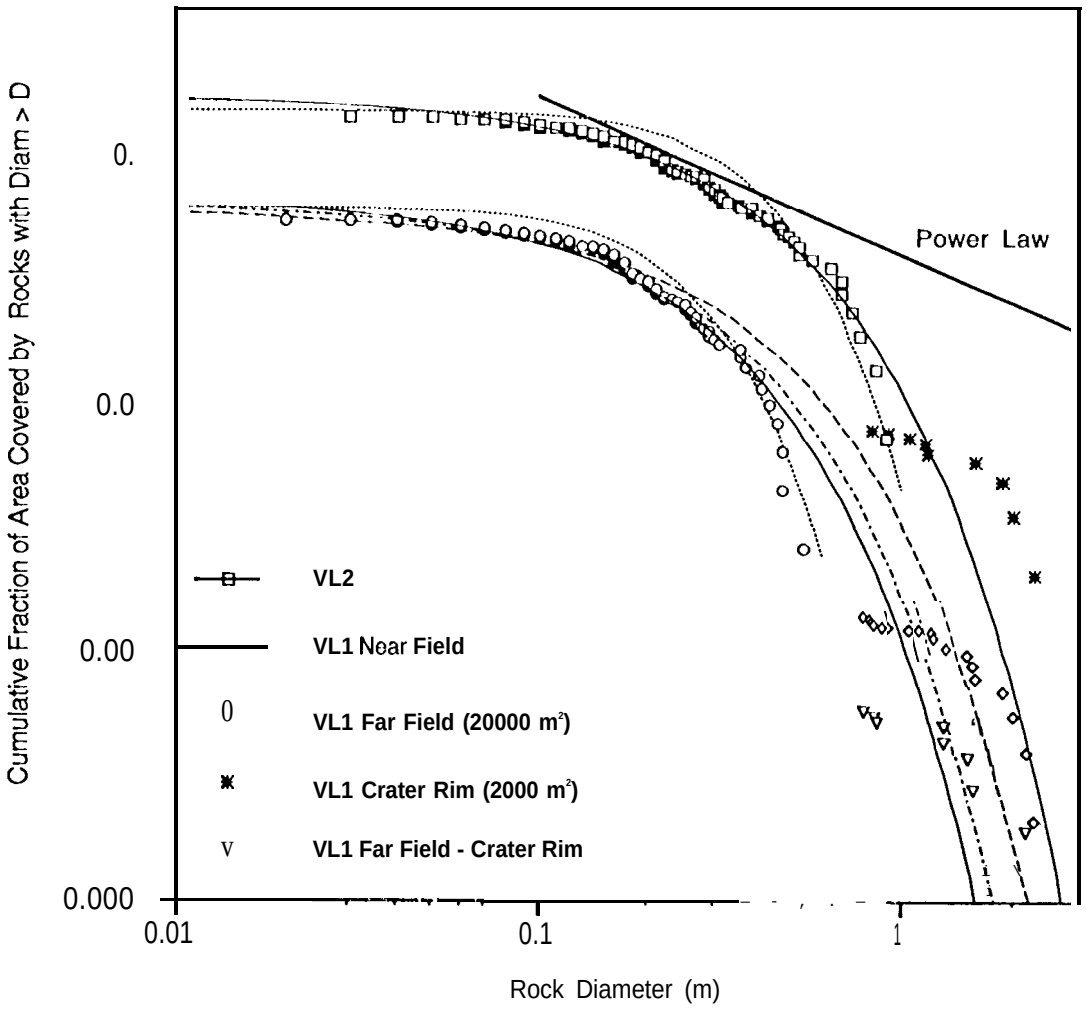
Cumulative Fraction of Area Covered by Rocks with Diam > D
0.
0.0
0.00
0.000
0.01
0.1
1
Rock Diameter (m)
Power Law
VL2
VL1 Near Field
VL1 Far Field (20000 m²)
VL1 Crater Rim (2000 m²)
VL1 Far Field - Crater Rim

Figure 4

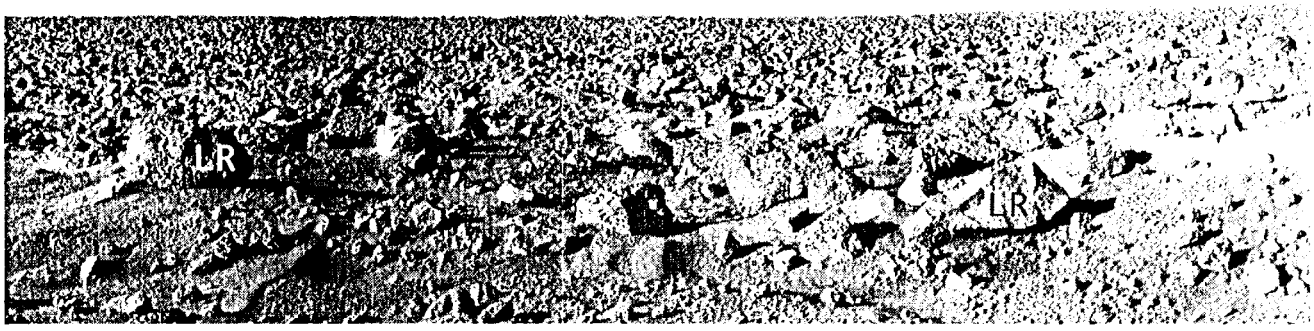

Figure 5

Figure 6

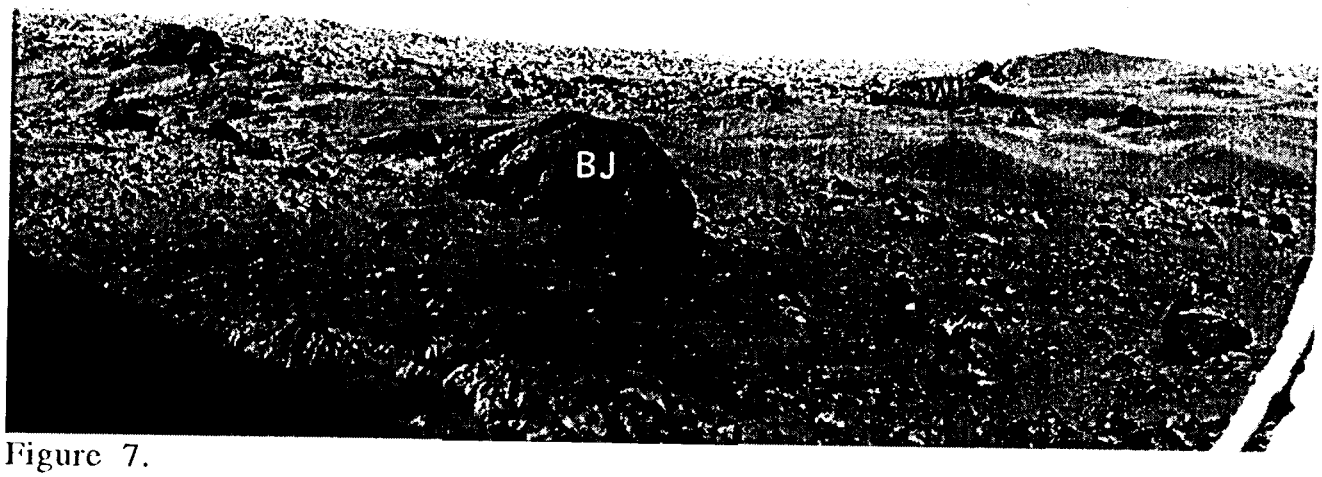

Figure 7.

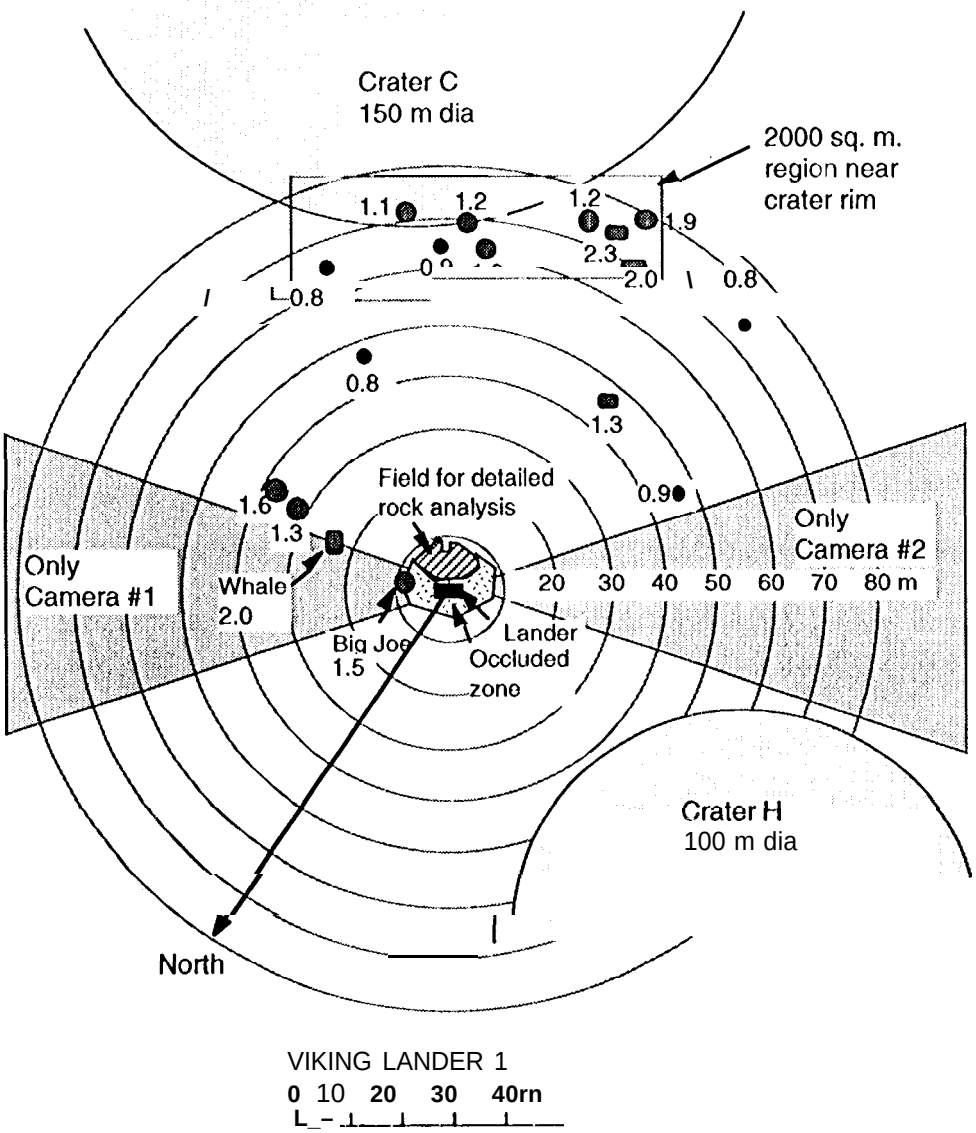
Crater C
150 m dia
2000 sq. m.
region near
crater rim
1.1
1.2
1.2
1.9
2.3
2.0
0.8
0.8
0.8
1.3
0.9
1.6
1.3
Field for detailed
rock analysis
Only
Camera #1
Whale
2.0
Only
Camera #2
20 30 40 50 60 70 80 m
Big Joe
1.5
Lander
Occluded
zone
Crater H
100 m dia
North
VIKING LANDER 1
0 10 20 30 40rn

Figure 8

Figure 9.

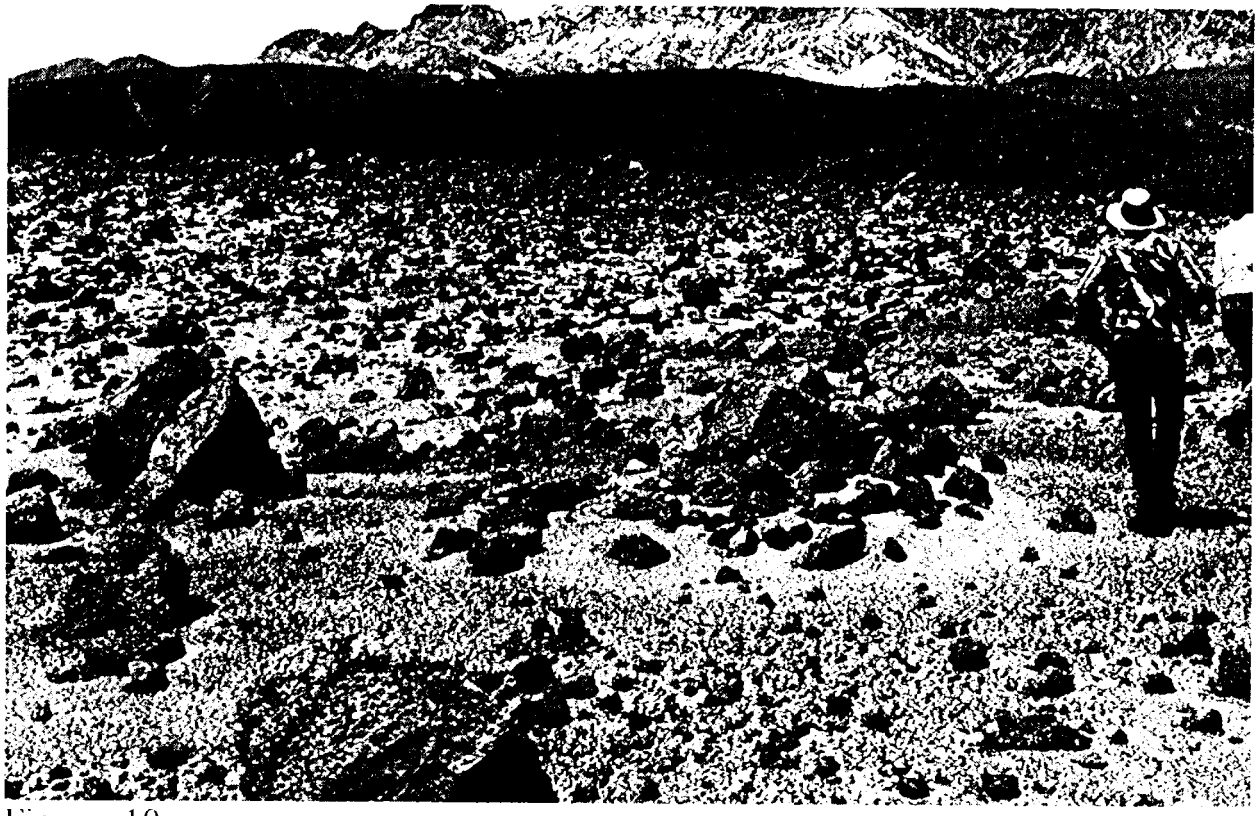

Figure 10.

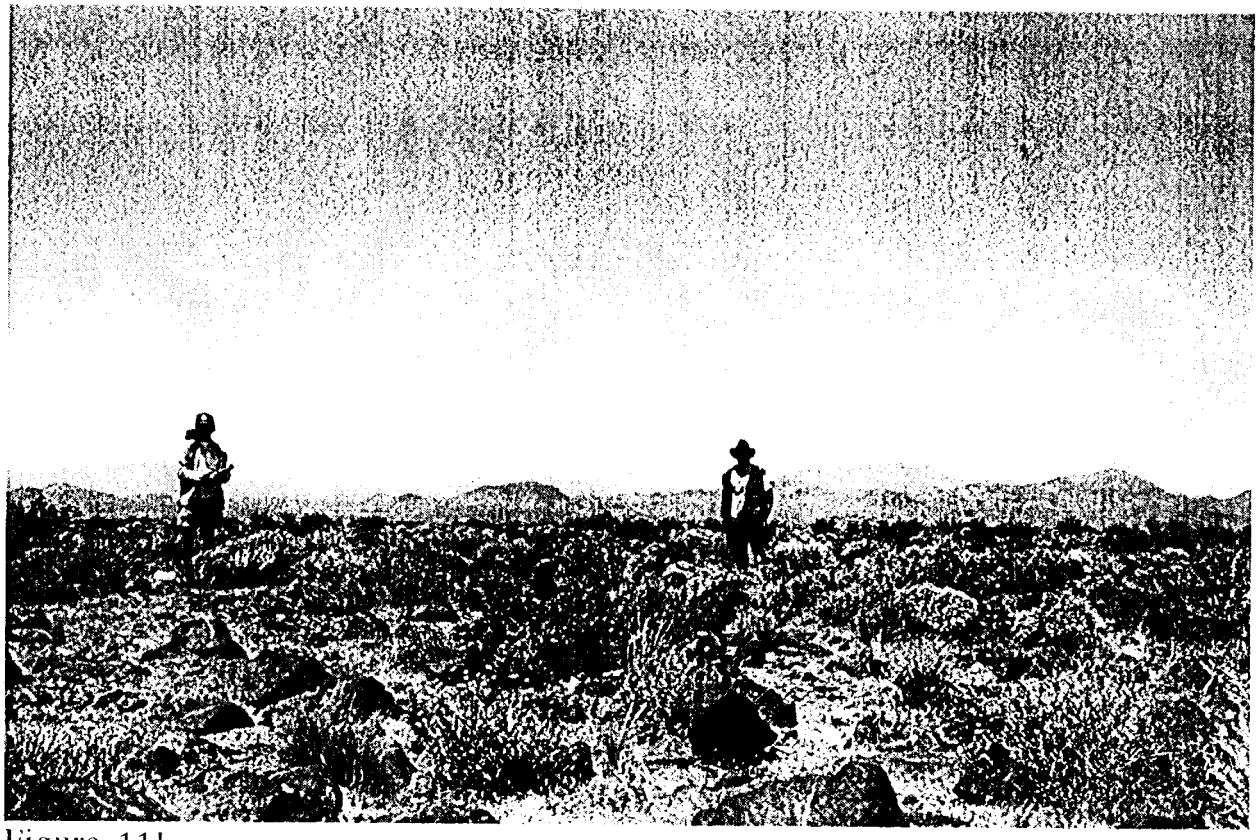

Figure 11!

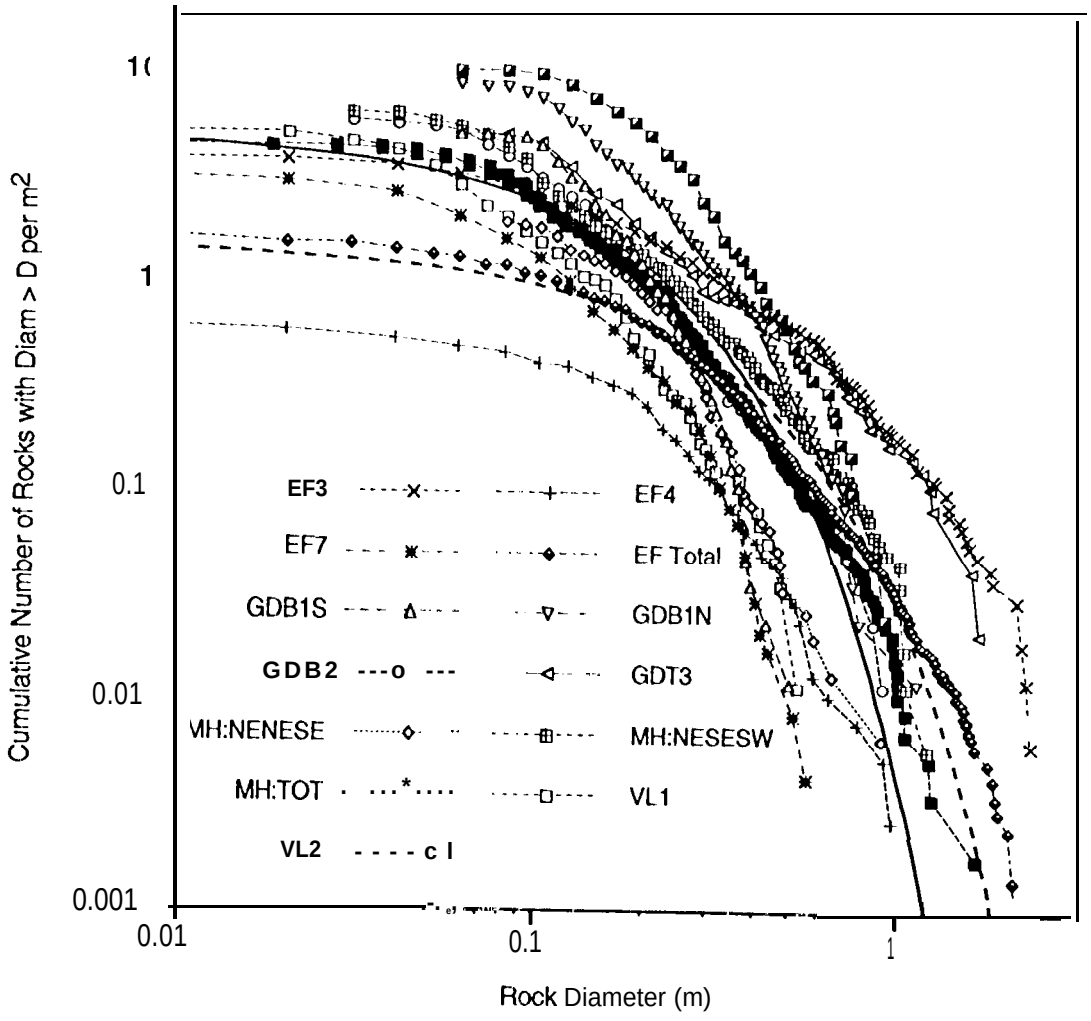
Cumulative Number of Rocks with Diam > D per m2
10
1
0.1
0.01
0.001
0.01
0.1
1
Rock Diameter (m)
EF3
EF4
EF7
EF Total
GDB1S
GDB1N
GDB2
GDT3
MH:NENESE
MH:NESESW
MH:TOT
VL1
VL2

Figure 12

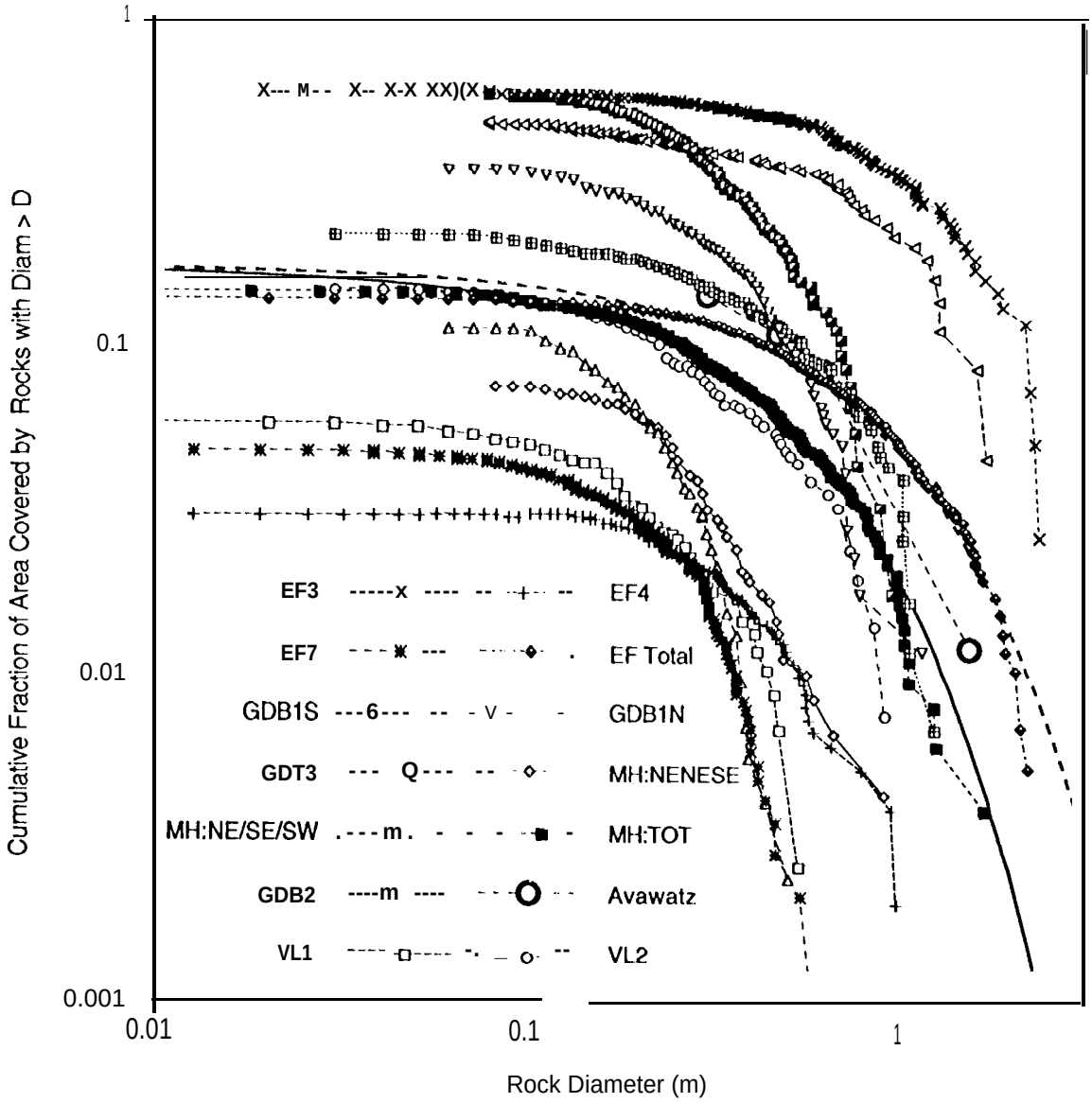
Cumulative Fraction of Area Covered by Rocks with Diam > D
1
0.1
0.01
0.001
0.01
0.1
1
Rock Diameter (m)
EF3
EF4
EF7
EF Total
GDB1S
GDB1N
GDT3
MH:NENESE
MH:NE/SE/SW
MH:TOT
GDB2
Avawatz
VL1
VL2

Figure 13

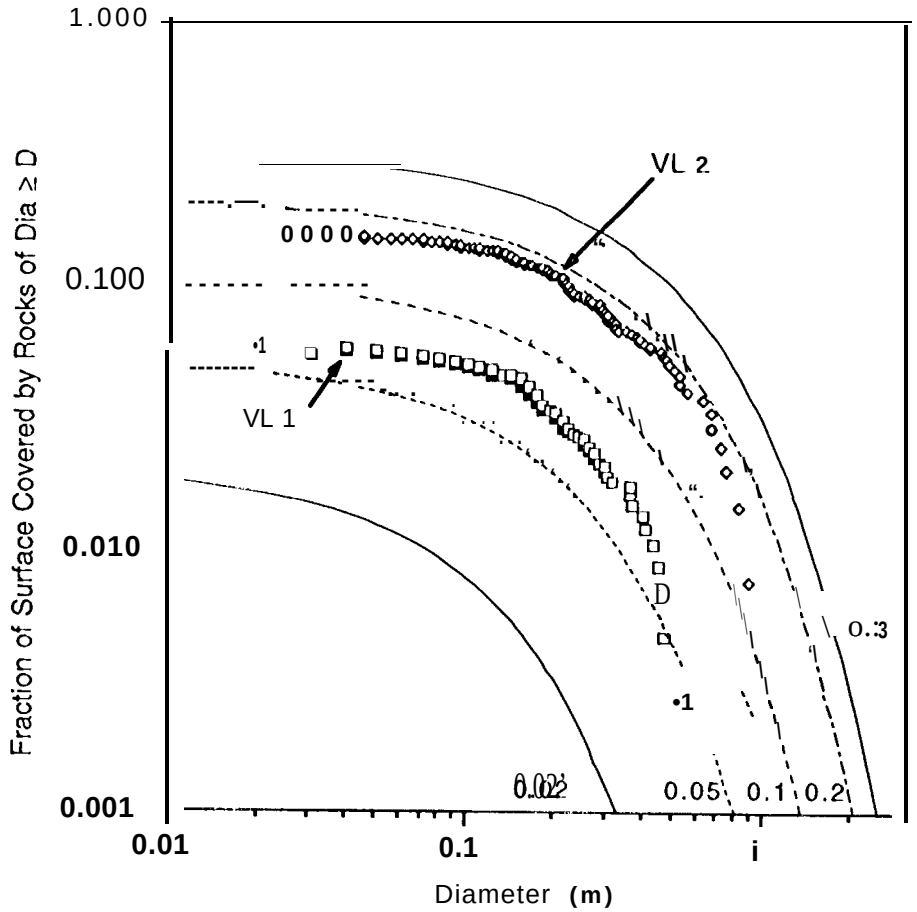
1.000
0.100
0.010
0.001
Fraction of Surface Covered by Rocks of Dia ≥ D
VL 2
VL 1
0.01
0.1
Diameter (m)
0.05
0.1
0.2
0.3

Figure 14

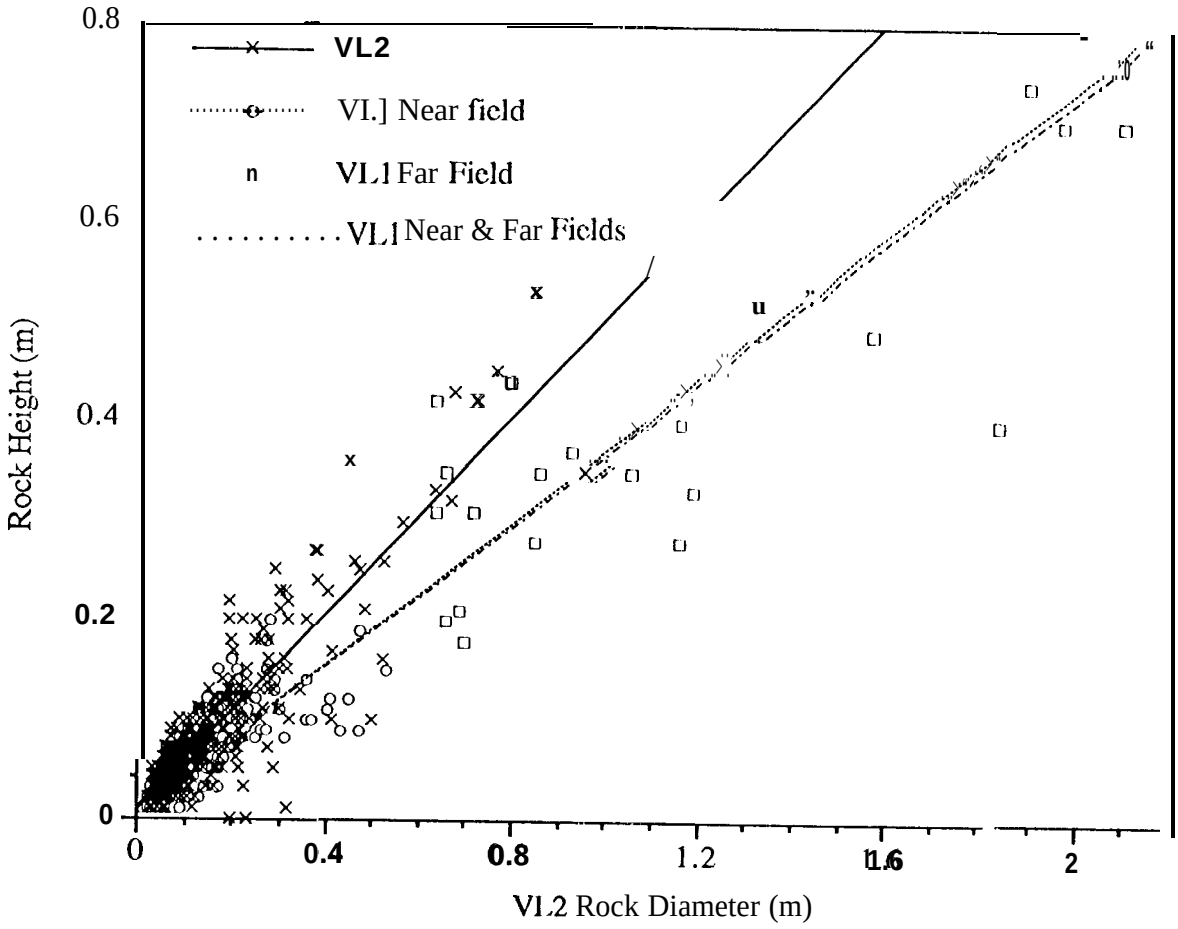
VL2
VI.] Near field
VL1 Far Field
VL1 Near & Far Fields
Rock Height (m)
0.8
0.6
0.4
0.2
0
0
0.4
0.8
1.2
1.6
2
VL2 Rock Diameter (m)

Figure 15

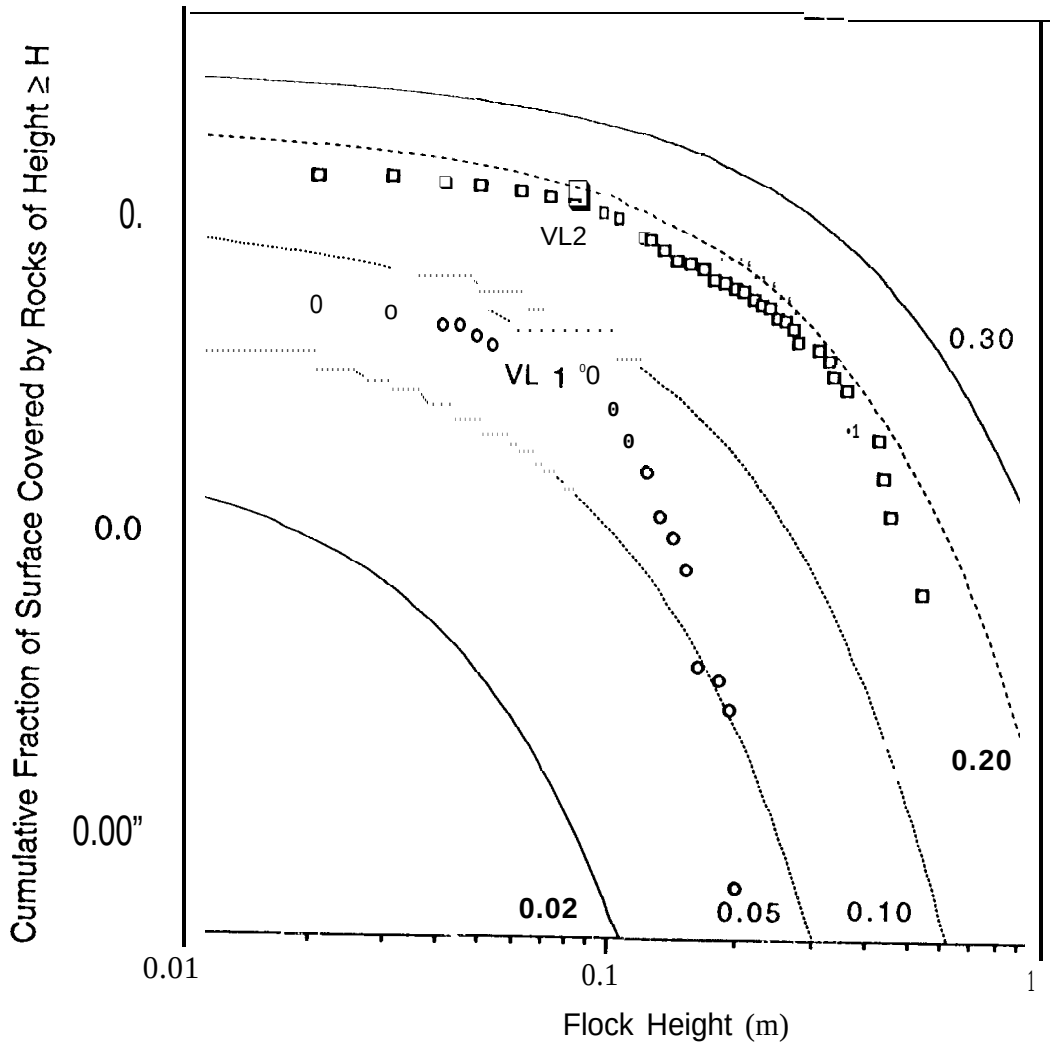
Cumulative Fraction of Surface Covered by Rocks of Height ≥ H
0.
0.0
0.00"
VL2
VL 1
0.30
0.20
0.10
0.05
0.02
0.01
0.1
1
Flock Height (m)

Figure 16